Available online at www.sciencedirect.com
SCIENCE DIRECT®
Journal of Organometallic Chemistry 669 (2003) 149–153
Journal of Organometallic Chemistry
www.elsevier.com/locate/jorganchem

Secondary bonding in *para*-substituted diphenyltellurium dichlorides ($(p\text{-}XC_6H_4)_2TeCl_2$ ($X = H$, Me, MeO) probed by ^{125}Te MAS NMR spectroscopy. Crystal and molecular structure of $(p\text{-}MeC_6H_4)_2TeCl_2$

Jens Beckmann*, Dainis Dakternieks, Andrew Duthie, Naomi A. Smith

Centre for Chiral and Molecular Technologies, Deakin University, Geelong 3217, Australia

Received 25 November 2002; received in revised form 8 January 2003; accepted 9 January 2003

Abstract

The solid-state structures of the previously known *para*-substituted diphenyltellurium dichlorides, $(p\text{-}XC_6H_4)_2TeCl_2$ (X = H (**1**), Me (**2**), MeO (**3**)) were investigated by ^{125}Te MAS NMR spectroscopy and in case of **2** by single crystal X-ray diffraction. The ^{125}Te-NMR shielding anisotropy (SA) was studied by tensor analyses based on relative intensities of the observed spinning sidebands. Solid-state NMR parameters, namely the isotropic chemical shift (δ_{iso}), anisotropy (ζ) and asymmetry (η), were discussed in relation to the molecular structures established by X-ray crystallography. The asymmetry (η) was found to be particularly sensitive to structural differences stemming mostly from the diverse secondary Te···Cl interactions, but no correlation with geometric parameters could be established.

Keywords: Secondary bonding; Tellurium; ^{125}Te MAS NMR spectroscopy; X-ray crystallography

1. Introduction

In recent years there has been an increasing interest in supramolecular aspects of organometallic structural chemistry [1]. In this regard organotellurium compounds have received special attention owing to their inherent propensity to form non-covalent Te···X bonds (X = F, Cl, Br, I, N, O, S) for which the term secondary interactions was introduced by Alcock [2]. In a recent survey the supramolecular structures of diorganotellurium(IV) dihalides were compiled and the influence of the various primary and secondary Te–X interactions on the geometry of the tellurium atoms investigated in great detail [3].

Solid-state NMR spectroscopy of heavy elements with spin 1/2 nuclei, such as ^{183}W, ^{195}Pt, ^{199}Hg, ^{205}Tl, ^{119}Sn, ^{207}Pb or ^{125}Te, is usually associated with very large shielding anisotropies (SA), which are intimately related to the coordination number, shape and symmetry of the investigated element [4]. The use of magic angle spinning (MAS) in solid-state NMR spectroscopy partly eliminates the effects of shielding anisotropy and allows the acquisition of solid-state NMR spectra with narrow signals and good signal-to-noise ratios in reasonable times. These signals may be accompanied by spinning sideband manifolds, which resemble the shape and width of the original static spectra and therefore allow the determination of the three principal tensor components of the shielding anisotropy based on the relative signal intensities within the spinning sideband manifolds [5–7]. The results of tensor analysis have been frequently used to correlate ^{119}Sn MAS NMR parameters with structural features in organotin compounds [8], for instance to probe the hypervalency of triorganotin fluorides, R_3SnF (R = alkyl, aryl), and related compounds [9–14]. To the best of our knowledge, similar systematic studies have not yet been reported in organotellurium chemistry. In fact, we are aware of only two works utilizing ^{125}Te MAS NMR spectroscopy including tensor analyses, namely to investigate triorganotellurium compounds, R_3TeX (R = Me, Ph; X = Cl, Br, I, NO_3) [15,16].

---

* Corresponding author. Tel.: +61-3-5227-1416; fax: +61-3-5227-1040.
E-mail address: beckmann@deakin.edu.au (J. Beckmann).

0022-328X/03/$ - see front matter © 2003 Elsevier Science B.V. All rights reserved.
doi:10.1016/S0022-328X(03)00005-6

In the present work we investigated the previously reported *para*-substituted diphenyltellurium dichlorides, (p-$XC_6H_4)_2TeCl_2$ (X = H (**1**), Me (**2**), MeO (**3**)) by ^{125}Te MAS NMR spectroscopy and compare the results with the supramolecular structures established by X-ray crystallography.

2. Discussion

The *para*-substituted diphenyltellurium dichlorides, (p-$XC_6H_4)_2TeCl_2$ (X = H (**1**), Me (**2**), MeO (**3**)) were prepared by the reaction of $TeCl_4$ with the appropriate benzene derivatives [17].

2.1. Crystal and molecular structure of (p-$MeC_6H_4)_2TeCl_2$ (**2**)

The crystal structure of **2** consists of two crystallographically independent (p-$MeC_6H_4)_2TeCl_2$ molecules that are associated with symmetry related pairs by secondary Te···Cl interactions as shown in Fig. 1; selected bond lengths and angles are collected in Table 1. This arrangement closely resembles the structural motif found for (p-$MeOC_6H_4)_2TeCl_2$ (**3**), but differs substantially from the polymeric arrangement of Ph_2TeCl_2 (**1**) in the solid state. Taking into account the steric demand of the stereochemically active lone pair, the geometry of Te1 and Te2 is best described as distorted pentagonal bipyramidal (type **A**, Chart 1). In agreement with the VSEPR theory the two primary Cl atoms occupy the apical sites, whereas the two C atoms, the lone pair and two secondary (intermolecular) Cl

Table 1
Selected bond lengths (Å) and bond angles (°) for **2**

Bond lengths			
Te1–Cl1	2.492(2)	Te1–Cl2	2.538(2)
Te1–Cl3	3.683(4)	Te1–Cl4a	3.702(2)
Te1–C10	2.129(3)	Te1–C20	2.103(3)
Te2–Cl3	2.521(2)	Te2–Cl4	2.502(2)
Te2–Cl2	3.816(4)	Te2–Cl2a	3.667(2)
Te2–C30	2.113(3)	Te2–C40	2.102(3)
Bond angles			
Cl1–Te1–Cl2	174.85(3)	Cl1–Te1–C10	90.95(8)
Cl1–Te1–C20	87.66(8)	Cl2–Te1–C10	91.53(8)
Cl2–Te1–C20	87.51(8)	C10–Te1–C20	98.71(11)
Cl3–Te2–Cl4	176.36(3)	Cl3–Te2–C30	88.68(8)
Cl3–Te2–C40	88.94(8)	Cl4–Te2–C30	89.06(8)
Cl4–Te2–C40	88.61(9)	C30–Te2–C40	99.36(11)

Symmetry operation used to generate equivalent atoms: a = 2−x, 1−y, 1−z.

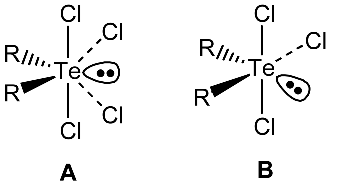

Chart 1.

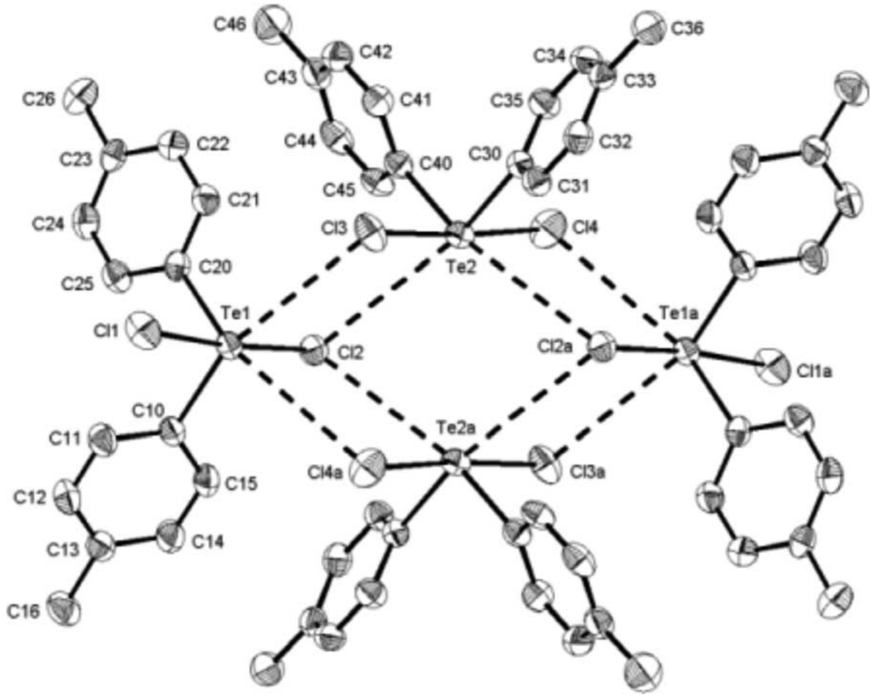

Fig. 1. Perspective view (DIAMOND) of the two pairs of crystallographically independent molecules of (p-$MeC_6H_4)_2TeCl_2$ (**2**) associated by secondary Te···Cl interactions (broken lines) showing 30% probability displacement ellipsoids and the crystallographic numbering scheme (symmetry operation used to generate equivalent atoms: a = 2−x, 1−y, 1−z).

atoms are situated in the equatorial positions. According to a recent survey this 5+2 coordination geometry is the most frequently encountered for diorganotellurium dihalides (type **A**, Chart 1) [3]. In fact, a very similar geometry was also found for the two independent Te sites in the crystal structure of (p-MeOC$_6$H$_4$)$_2$TeCl$_2$ (**3**) [18]. By contrast, Ph$_2$TeCl$_2$ (**1**) revealed only a 5+1 coordination geometry in the solid state (type **B**, Chart 1) [19]. An important difference of the Te sites of **2** is found in the coordination number of the apical Cl atoms, which is reflected in their primary Te–Cl bond lengths. At Te1, the Cl2 atom shows a 1+2 coordination (Te1–Cl2: 2.538(2) Å), whereas Cl1 is not involved in any secondary interactions (Te1–Cl1: 2.492(2) Å). By contrast, at Te2, both Cl3 and Cl4 show a 1+1 coordination (Te2–Cl3: 2.521(2) Å and Te2–Cl4: 2.502(2) Å). Thus, the Te–Cl bond length increases with the coordination number of the Cl atoms. Similar observations were also made for Ph$_2$TeCl$_2$ (**1**; Te1–Cl1: 2.528(3) Å, Te1–Cl2: 2.481(2) Å) [19] and (p-MeOC$_6$H$_4$)$_2$TeCl$_2$ (**3**; Te1–Cl1: 2.517(34) Å, Te1–Cl2a: 2.514(34) Å, Te2–Cl3: 2.474(34) Å, Te2–Cl4: 2.588(34) Å) [18]. The apical Cl–Te–Cl bond angles of (p-MeC$_6$H$_4$)$_2$TeCl$_2$ (**2**; 174.85(3) and 176.36(3)°) are very similar to those of Ph$_2$TeCl$_2$ (**1**; 175.51(0)°) and (p-MeOC$_6$H$_4$)$_2$TeCl$_2$ (**3**; 177.88(2) and 178.61 (2)°). The C–Te–C bond angles of **2** (98.71(11) and 99.36(11)°) are in close agreement with those of Ph$_2$TeCl$_2$ (**1**; 99.01(29)°) [19] and (p-MeOC$_6$H$_4$)$_2$TeCl$_2$ (**3**; 97.00(2) and 95.93(2)°) [18].

2.2. *^{125}Te-NMR spectroscopy*

Compounds **1**–**3** were recrystallized from the solvents used to grow the single crystals for the X-ray experiments to minimize confusion with possible polymorphs [18,19]. The ^{125}Te-NMR chemical shifts of **1**–**3** obtained in solution (CDCl$_3$) and in the solid-state are collected in Table 2. Since diorganotellurium dichlorides comprise monomers in solution, a comparison of the ^{125}Te-NMR signals in CDCl$_3$ ranging from 919.7 to 933.1 ppm reveals a small influence on the ^{125}Te-NMR chemical shifts by the organic substituents. A first examination of the ^{125}Te MAS NMR spectra of **1**–**3** shows that the number of signals is in all cases fully consistent with the number of crystallographically independent Te sites as established by X-ray diffraction; the spectra are shown in Figs. 2–4. By contrast, ^{125}Te Mössbauer spectroscopy appears to be less sensitive to minute structural differences, e.g. for (p-MeC$_6$H$_4$)$_2$TeCl$_2$ (**2**) only one set of parameters (isomeric shift and quadrupole splitting) was obtained [20]. The ^{125}Te MAS NMR chemical shifts of **1**–**3** range from 900.0 to 1001.7 ppm and are reasonably close to the values observed in CDCl$_3$ solution. The isotropic chemical shifts were accompanied by sets of spinning sidebands that were utilized to perform tensor analyses [5–7], the results of which are collected in Table 2. The anisotropies (ζ) of **1**–**3** lie in a comparatively small range between 232 and 313 ppm, which precluded reliable correlations with geometrical features, e.g. the coordination number of the Te sites. Despite the very similar coordination geometries of the Te atoms in **1**–**3**, the asymmetry (η) surprisingly adopts values varying from 0.50 to 0.95. However, no correlation of asymmetry (η) with geometrical parameters, e.g. Te–Cl bond lengths or C–Te–C bond angles, could be established. By comparison of the structures of **1**–**3** derived from X-ray crystallography the anisotropy (ζ) and asymmetry (η) of Ph$_2$TeCl$_2$ (**1**) might be expected to be somewhat different from those of (p-MeC$_6$H$_4$)$_2$TeCl$_2$ (**2**) and (p-MeOC$_6$H$_4$)$_2$TeCl$_2$ (**3**), however, the parameters observed lie midway between those of **2** and **3**.

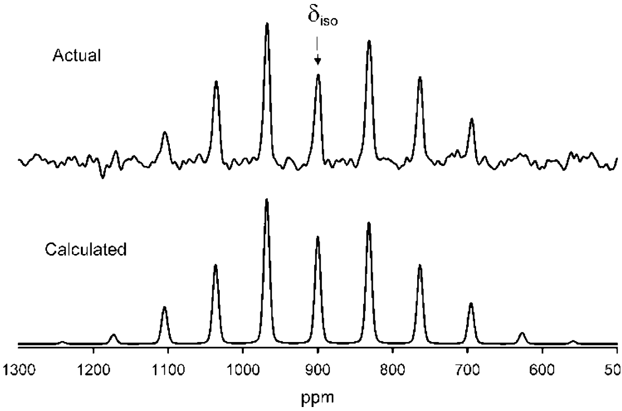

Fig. 2. Experimentally determined and iteratively fitted ^{125}Te MAS NMR spectrum (MAS frequency 8600 kHz) of Ph$_2$TeCl$_2$ (**1**).

Table 2
Solution and solid-state ^{125}Te-NMR parameters of **1**–**3**

Compound	δ_{CDCl3}	δ_{iso}	ζ	η	σ_{11}	σ_{22}	σ_{33}
(C$_6$H$_5$)$_2$TeCl$_2$ (**1**)	919.7	900.0	273	0.70	−1132	−941	−627
(p-MeC$_6$H$_4$)$_2$TeCl$_2$ (**2**)	924.8	938.3	259	0.95	−1191	−945	−679
		951.5	313	0.50	−1108	−1004	−743
(p-MeOC$_6$H$_4$)$_2$TeCl$_2$ (**3**)	933.1	979.4	232	0.60	−1165	−1026	−747
		1001.7	232	0.55	−1182	−1054	−770

δ_{iso} (ppm) $= -\sigma_{iso} = -(\sigma_{11}+\sigma_{22}+\sigma_{33})/3$; ζ (ppm) $= \sigma_{33}-\sigma_{iso}$ and $\eta = (\sigma_{22}-\sigma_{11})/(\sigma_{33}-\sigma_{iso})$ where σ_{11}, σ_{22} and σ_{33} (ppm) are the principal tensor components of the shielding anisotropy (SA), sorted as follows $|\sigma_{33}-\sigma_{iso}| > |\sigma_{11}-\sigma_{iso}| > |\sigma_{22}-\sigma_{iso}|$.

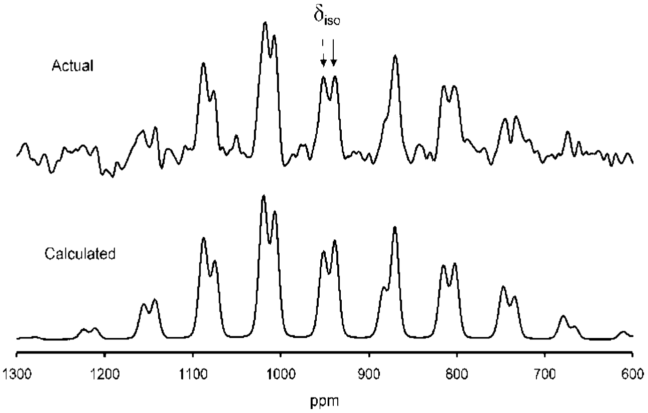

Fig. 3. Experimentally determined and iteratively fitted ^{125}Te MAS NMR spectrum (MAS frequency 8600 kHz) of (p-MeC$_6$H$_4$)$_2$TeCl$_2$ (**2**).

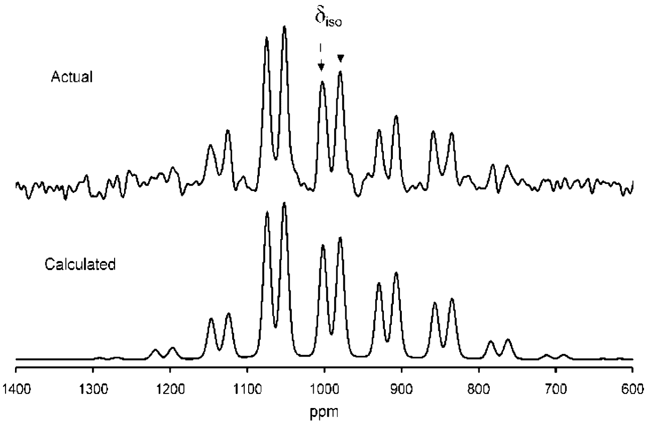

Fig. 4. Experimentally determined and iteratively fitted ^{125}Te MAS NMR spectrum (MAS frequency 9100 kHz) of (p-MeOC$_6$H$_4$)$_2$TeCl$_2$ (**3**).

3. Experimental

3.1. ^{125}Te-NMR spectroscopy

Solution ^{125}Te-NMR spectra were measured in CDCl$_3$ at 85.39 MHz using a JEOL GX 270 MHz NMR spectrometer and were referenced against Me$_2$Te. The ^{125}Te MAS NMR spectra were obtained at 126.26 MHz using a JEOL Eclipse Plus 400 MHz NMR spectrometer equipped with a high-speed locked 6 mm rotor operating at spinning frequencies between 7 and 10 kHz (experimental conditions: pulse 6 μs (40°), recycle delay 180 s). Typically 500–1000 transitions were accumulated to obtain signal-to-noise ratios adequate for the tensor analyses. Preliminary attempts to reduce the acquisition times by applying a CP-MAS pulse sequence were unsuccessful. The isotropic chemical shifts δ_{iso} were determined by comparison of two acquisitions measured at sufficiently different spinning frequencies and were referenced against Me$_2$Te using solid Te(OH)$_6$ as the secondary reference (δ_{iso} 692.2/685.5) [15]. The tensor analyses were performed using DMFIT 2002 and are based on relative intensities of the spinning sideband intensities [21]. The definitions of δ_{iso}, ζ, η, σ_{iso}, σ_{11}, σ_{22} and σ_{33} are given in the footnote of Table 2.

3.2. Crystal structure determination of (p-MeC$_6$H$_4$)$_2$TeCl$_2$ (2)

Single crystals of (p-MeC$_6$H$_4$)$_2$TeCl$_2$ (**2**) suitable for X-ray crystallography were obtained by slow evaporation of a CH$_2$Cl$_2$–hexane solution. Crystal data and structure solution of **2** at $T = 293(2)$ K: C$_{14}$H$_{14}$TeCl$_2$, $M_r = 380.80$, monoclinic, $P2_1/n$, crystal dimensions: $0.10 \times 0.25 \times 0.25$ mm^3, $a = 16.518(2)$, $b = 10.1828(12)$, $c = 17.511(2)$ Å, $\beta = 94.356(2)°$, $V = 2936.83(60)$ Å^3, $Z = 8$, $\rho_{\text{calc}} = 1.722$ Mg m^{-3}, $F(000) = 1472$, $\mu = 2.366$ mm^{-1}. Intensity data were collected on Bruker SMART Apex CCD diffractometer fitted with Mo–K$_\alpha$ radiation (graphite crystal monochromator, $\lambda = 0.71073$ Å) to a maximum of $\theta_{\max} = 27.53°$ via ω scans (completeness 94.4% to $\theta_{\max}$). Data were reduced and corrected for absorption using the programs SAINT and SADABS [22]. The structure was solved by direct methods and difference Fourier synthesis using SHELX-97 implemented in the program WINGX 2002 [23]. Full-matrix least-squares refinement on F^2, using all data, was carried out with anisotropic displacement parameters applied to all non-hydrogen atoms. Hydrogen atoms were included in geometrically calculated positions using a riding model and were refined isotropically. The weighting scheme employed was of the type $w = [\sigma^2(F_o^2) + (0.0423P)^2 + 0.4300P]^{-1}$ where $P = (F_o^2 + 2F_c^2)/3$. $R_1 = 0.0302$ for 5433 $[I > 2\sigma(I)]$ reflections and $wR_2 = 0.0764$ for 6376 independent reflections; GooF = 1.018. The max. and min. residual electron densities were 0.652/−0.395 e Å^{-3}.

4. Supplementary material

Crystallographic data (excluding structure factors) for the structural analysis have been deposited with the Cambridge Crystallographic Data Centre, CCDC no. 200100 for compound **2**. Copies of this information may be obtained free of charge from The Director, CCDC, 12 Union Road, Cambridge CB2 1EZ, UK (Fax: +44-1223-336033; e-mail: deposit@ccdc.cam.ac.uk or www: http://www.ccdc.cam.ac.uk).

Acknowledgements

The Australian Research Council (ARC) is thanked for financial support. Dr. Jonathan White (Melbourne

University) is gratefully acknowledged for the X-ray crystallography data collection.

References

[1] I. Haiduc, F.T. Edelmann, Supramolecular Organometallic Chemistry, VCH, Weinheim, 1999.
[2] I. Haiduc, J. Zukerman-Schpector, Phosphorus Sulfur Silicon 171–172 (2001) 171.
[3] J. Zukerman-Schpector, I. Haiduc, Phosphorus Sulfur Silicon 171–172 (2001) 73.
[4] A. Sebald, in: P. Diehl, E. Fluck, H. Günther, R. Kosfeld, J. Seeling (Eds.), Solid-State NMR II Inorganic Matter. NMR Basic Principles and Progress, vol. 31, Spinger, Heidelberg, 1994, p. 91.
[5] M.M. Maricq, J.S. Waugh, J. Chem. Phys. 70 (1979) 3300.
[6] J. Herzfeld, A.E. Berger, J. Chem. Phys. 73 (1980) 6021.
[7] J. Herzfeld, X. Chen, in: D.M. Grant, R.K. Harris (Eds.), Encyclopedia of Nuclear Magnetic Resonance, vol. 7, Wiley, Chichester, 1996, p. 4362.
[8] R.K. Harris, S.E. Lawrence, S.W. Oh, V.G. Kumar Das, J. Mol. Struct. 347 (1995) 309.
[9] H. Bai, R.K. Harris, H. Reuter, J. Organomet. Chem. 408 (1991) 167.
[10] H. Bai, R.K. Harris, J. Magn. Reson. 96 (1992) 24.
[11] Y.W. Kim, A. Labouriau, C.M. Taylor, W.L. Earl, L.G. Werbelow, J. Phys. Chem. 98 (1994) 4919.
[12] J.C. Cherryman, R.K. Harris, J. Magn. Reson. 128 (1997) 21.
[13] J. Beckmann, D. Dakternieks, A. Duthie, E.R.T. Tiekink, J. Organomet. Chem. 648 (2002) 204.
[14] J. Beckmann, D. Horn, K. Jurkschat, F. Rosche, M. Schürmann, U. Zachwieja, D. Dakternieks, A. Duthie, A.E.K. Lim, Eur. J. Inorg. Chem. 8 (2003) 164.
[15] M.J. Collins, J.A. Ripmeester, J.F. Sawyer, J. Am. Chem. Soc. 109 (1987) 4113.
[16] M.J. Collins, J.A. Ripmeester, J.F. Sawyer, J. Am. Chem. Soc. 110 (1988) 8583.
[17] J. Bergman, Tetrahedron 28 (1972) 3323.
[18] R.K. Chadha, J.E. Drake, Acta Crystallogr. Sect. C 40 (1984) 1349.
[19] N.W. Alcock, W.D. Harrison, J. Chem. Soc. Dalton Trans. (1982) 251.
[20] F.J. Berry, E.H. Kustan, B.C. Smith, J. Chem. Soc. Dalton Trans. (1975) 1323.
[21] D. Massiot, F. Fayon, M. Capron, I. King, S. Le Calvé, B. Alonso, J.O. Durand, B. Bujoli, Z. Gan, G. Hoatson, Magn. Res. Chem. 40 (2002) 70.
[22] SMART, SAINT and SADABS, Siemens Analytical X-ray Instruments Inc., Madison, WI, 1999.
[23] L.J. Farrugia, J. Appl. Crystallogr. 20 (1997) 565.